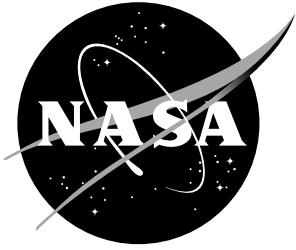


Corrosion Studies of Wrought and Cast NASA-23 Alloy

M.D. Danford



Corrosion Studies of Wrought and Cast NASA-23 Alloy

M.D. Danford
Marshall Space Flight Center • MSFC, Alabama

TABLE OF CONTENTS

1. INTRODUCTION	1
2. THE SCANNING REFERENCE ELECTRODE TECHNIQUE (SRET)	2
3. EXPERIMENTAL PROCEDURES	3
3.1. Electrochemical Methods	3
4. RESULTS AND DISCUSSION	5
4.1 SRET Experiments	5
4.2 Corrosion Rate Measurements	5
5. CONCLUSIONS	10
REFERENCES	11

LIST OF FIGURES

1.	The scanning reference electrode system	2
2.	Initial localized corrosion in cast NASA-23 alloy	6
3.	Localized corrosion in cast NASA-23 alloy after 1 hr	6
4.	Initial localized corrosion in wrought NASA-23 alloy	7
5.	Localized corrosion in wrought NASA-23 alloy after 1 hr	7
6.	Localized corrosion in wrought NASA-23 alloy after 1 hr	8
7.	Localized corrosion in wrought NASA-23 alloy after 2 hr	8
8.	Circuit representing alternate-current impedance response for bare metals	9
9.	Observed corrosion for wrought and cast NASA-23 alloy	10

TECHNICAL PAPER

CORROSION STUDIES OF WROUGHT AND CAST NASA-23 ALLOY

1. INTRODUCTION

NASA-23 is a relatively new aerospace alloy developed at Marshall Space Flight Center, using Incoloy 903 as a point of departure. Incoloy 903 was selected as a starting point because of its superior hydrogen resistance. The primary element in which a major change was made was Chromium (Cr), which was increased from 1 percent to about 10 percent to improve oxidation resistance. The new alloy would not exhibit the poor oxidation characteristics of Incoloy 903, but would retain its excellent hydrogen resistance. NASA-23 is a face-centered cubic alloy with a cell parameter of 3.60 Å, similar to Incoloy 903 and other face-centered cubic metal alloys. Possible uses include applications in the proposed Reusable Launch Vehicle (RLV) which will be developed starting the year 2000. In this work, electrochemical methods were employed with the purpose of generating additional information concerning the corrosion phenomenon, and making an addition to the data base for NASA-23. The corrosion characteristics of NASA-23 were studied in 1994 using the stress corrosion technique,¹ where it was found that the new alloy has excellent corrosion resistance. The relatively new scanning reference electrode technique (SRET) was used in this study, along with the conventional direct-current polarization resistance (PR) technique²⁻⁵ and the electrochemical impedance spectroscopy (EIS).⁶

2. THE SCANNING REFERENCE ELECTRODE TECHNIQUE (SRET)

The SRET is a veritable “time machine” for corrosion studies, employing high corrosion rates coupled with corrosion maps of the sample as a function of time. The SRET instrument shown in figure 1 is commercially available from EG&G Princeton Applied Research Corporation (EG&G PARC). It has the capability to measure microgalvanic potentials close to the surface of materials, and allows in situ examination and quantification, on a microscopic scale, of electrochemical activity as it occurs. The SRET is microprocessor-controlled, and electrochemical potentials are measured by a special probe capable of translation in the x and y directions. The specimen, in the form of a cylinder, is held in a vertical position and rotated around the y axis. The scan is synchronized with a display monitor and the resultant data are shown in the form of either line scans (x direction only) or two-dimensional area maps (x and y directions). The width of the area maps (x direction) can be set at will using the zoom-in feature of the experimental setup. The height of the area maps (y direction) is set automatically by the control software according to the proper aspect ratio. Movement of the scanning probe during data collection is in the y direction. Direct measurement of surface potentials, showing anodic and cathodic areas, at discrete positions on the sample surface may be taken and stored for time-related studies. Because the minimum detectable signal (MDS) is of the order of 1 mA/cm^2 , a potential must be applied to the sample to increase the corrosion current to at least this level, accomplished by means of a separate potentiostat (EG&G Model 273A Potentiostat/Galvanostat) coupled to the SRET system.

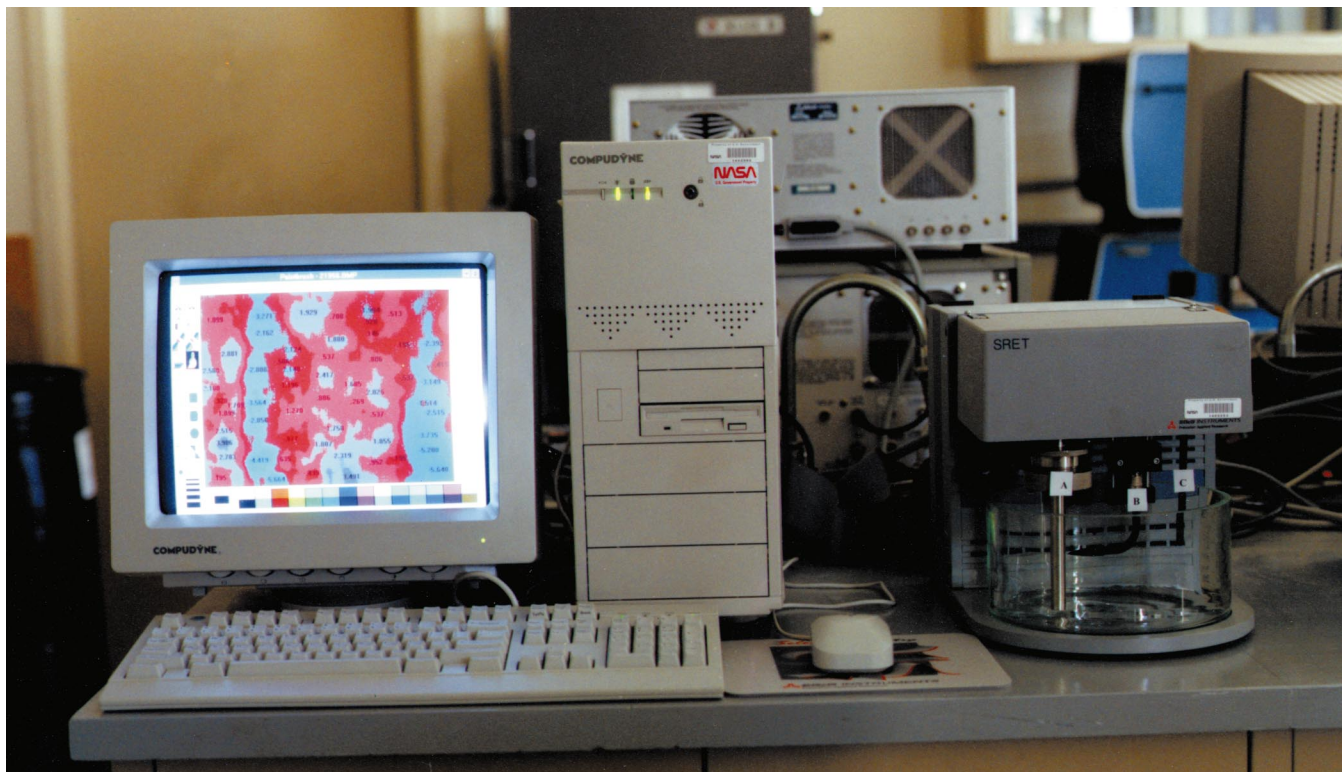


Figure 1. The scanning reference electrode system (A=Metal sample, B=Probe, C=Counter electrode).

3. EXPERIMENTAL PROCEDURES

Samples of both wrought and cast NASA-23 alloys were heat-treated in exactly the same way, since corrosion rates would probably be different if the heat treatments were not the same.

3.1 Electrochemical Methods

For SRET measurements, samples consisted of cylindrical metal rods 10.2 cm (4 in) long. For the cast NASA-23 alloy, the rod was 0.80 cm (0.316 in) in diameter, with a circumference of 2.52 cm (0.992 in), while the wrought alloy was 1.29 cm (0.51 in) in diameter, with a circumference of 4.05 cm (1.594 in). For each experiment, the test specimen was mounted in the collet of the SRET system and the probe, counter electrode, and reference electrode were placed in their proper positions in the machine. The probe was then driven to a position such that the point was approximately 0.5 to 1 mm from the metal cylinder, and the entire assembly was immersed in a corrosive medium consisting of a 3.5-percent sodium chloride (NaCl) solution. About a 5.1-cm (2-in) length of the metal sample rod was thus exposed to the corrosive medium. A potential noble to (more positive than) the normal corrosion potential (E_{corr}) was then applied to the metal sample rod. This applied potential was approximately the same for both the cast and wrought NASA-23, 1 V relative to E_{corr} and well above the MDS level. This potential resulted in a beginning corrosion rate which was about the same for both samples. During data collection the samples were rotated at 100 revolutions per minute (rpm). Map scans were taken, beginning and ending at equal distances from the zero point of the SRET system, starting with the initial status of the corrosion current density and applied potential, which was maintained at the same level throughout the experiment. The map for the cast alloy had a width of 2.5 cm (x direction) and a height of 1.9 cm (y direction); and for the wrought alloy, a width of 3 cm (x direction) and a height of 2.25 cm (y direction). An attempt was made to collect three maps for each sample, with a 1-hr delay between each (initial, 1 hr and 2 hr). The current density for the cast sample decayed too rapidly to permit collection of the final map, falling too far below the level for the MDS, while that for the wrought sample allowed the collection of all three maps. After data collection was completed, each map was displayed on the computer screen and the proper palette (color scheme) for display of map features (potentials for anodic and cathodic features) was obtained using software developed for this purpose. Potentials of the positive cathodic features and negative anodic features in millivolts were measured with the same software and typed on the maps in their appropriate places using other software.

Hardness and density were determined for each of the two samples (wrought and cast). The overall density for the cast sample was slightly higher (8.16 gm/cm³) than that for the wrought sample (8.11 gm/cm³). The hardness of the cast sample varied considerably from spot to spot (about R_c 24 to R_c 42), but the hardness was slightly higher for the cast sample (R_c 42.8) than that for the wrought sample (R_c 41.3) for the exposed surface areas (1 cm²) of the plates used in corrosion rate studies.

Data for the determination of the normal corrosion rates (at zero potential with respect to E_{corr}) for each of the samples exposed to 3.5 percent NaCl, a highly corrosive medium, were obtained using both the direct-current PR technique and the alternating current EIS technique, which is more sensitive. Current densities were sometimes too small to measure with the PR technique, especially in the case of the wrought NASA-23 material. For the PR method, data were collected using the EG&G instrumentation and software.

The potential applied to the specimen during the scan was varied from -20 mV to $+20$ mV on either side of the corrosion potential E_{corr} and the data points (current and potential) were recorded in $1/4$ -mV increments. The corrosion current at E_{corr} cannot be observed directly, but must be calculated. In this case, the data were analyzed using the program POLCURR.⁷ Flat plates, 3.81 cm (1.5 in) wide and 7.62 cm (3 in) long of each of the samples (wrought and cast NASA-23) were cleaned with dichloroethylene and alcohol. The plates were clamped in two separate flat cells manufactured by EG&G PARC. An area of 1 cm^2 for each plate was continuously exposed to a 3.5-percent NaCl solution. Corrosion currents for each were measured over a period of 10 days using either the PR or EIS method, with data for each sample being collected on alternate days. For the PR method, each measured result is the average of at least three separate determinations. The average time for each point was approximately 1 hr using this method. Silver/silver chloride reference electrodes were used in all cases.

For the EIS technique, measurements were taken in three frequency ranges, using the same EG&G PARC equipment plus the Model 5301 lock-in amplifier. The first two ranges, beginning at 0.001 Hz and 0.1 Hz, respectively, were obtained using the fast Fourier transform technique. Data in the third range, 5 to 10,000 Hz, were collected using the lock-in amplifier technique. The sequencing was performed using the autoexecute procedure, with all data merged to a single set for each determination. After collection, these data were processed and analyzed by computer using a suitable equivalent circuit model, which will be discussed later. Methods for analyzing the EIS data have been described elsewhere.⁶ Each EIS determination required approximately 3 hr to complete and was not repeated.

4. RESULTS AND DISCUSSION

4.1 SRET Experiments

The corrosion map scan for the cast NASA-23 alloy and for the initial and after-1-hr exposure to the corrosive medium are shown in figures 2 and 3, respectively. The map for the initial conditions (current and about 1 V potential) shows strong anodic and cathodic features, highly localized. The material, under these conditions, would be highly susceptible to pitting. However, the map, after a 1-hr exposure to the corrosive medium, shows much weaker features. The potential during this period was maintained at the same level (about 1 V), but the current had dropped to a point close to the MDS level. Thus, the initially strong features have passivated, and the corrosion rate is at a lower level. Also, the features are less highly localized and not as subject to pitting. A third map, after a 2-hr exposure, was not taken because the current would have been too far below the MDS level.

The corrosion map scans for the wrought NASA-23 alloy for the initial and after-1-hr exposure exposures to the corrosive medium are shown in figures 4 and 5, respectively. The map in figure 4 shows features which are not as highly localized, or as strong as, those in figure 5. Also, the features are not as highly localized or as strong as those in figure 2 for the cast alloy. The map in figure 5 shows extremely strong anodic and cathodic features, indicating a high susceptibility to deep pits in the metal. In figures 2 and 3, the corrosion maps for the cast alloy show a tendency toward a less active condition with time, while those for the wrought alloy show a tendency toward a more strongly localized corrosion mechanism with time, going from less active sites to strongly active sites. The maps in figures 6 (same as figure 5, repeated for easy comparison) and 7 show that there is not significant change in conditions between 2 hr and 3 hr of exposure. Thus, the corrosion mechanism has stabilized, and probably would not change a great deal at longer time intervals. Determinations of corrosion rates, which are measured at zero potential with respect to E_{corr} and are much lower than those observed under a potential of about 1 V, as applied for the SRET measurements, should be in accord with the mechanisms displayed in the map scans for the cast and wrought NASA-23 alloy (figs. 2–5). Measurements of corrosion rates for these samples are discussed in the next section.

4.2 Corrosion Rate Measurements

Both the PR and EIS methods were employed for measurements of normal corrosion rates, where there was no electric potential applied to the samples. All samples (flat plates of cast and wrought NASA-23) were continuously exposed to the 3.5-percent NaCl medium for a period of 10 days, during which measurements were made, as described previously.⁶ Corrosion rates for the wrought alloy were estimated primarily with the EIS technique. The equivalent circuit model used for the interpretation of the EIS data is shown in figure 8. Here, the charge transfer resistance, R_t , is equivalent to the polarization resistance, R_p , in the PR method. In the case of wrought NASA-23 alloy, currents were mostly too weak to be measured with the PR technique and required the EIS method, which is more sensitive. With the cast alloy, currents were generally high enough to measure with the PR technique, but measurements were made primarily using the EIS technique so that measurements for both the cast and wrought samples could be compared.

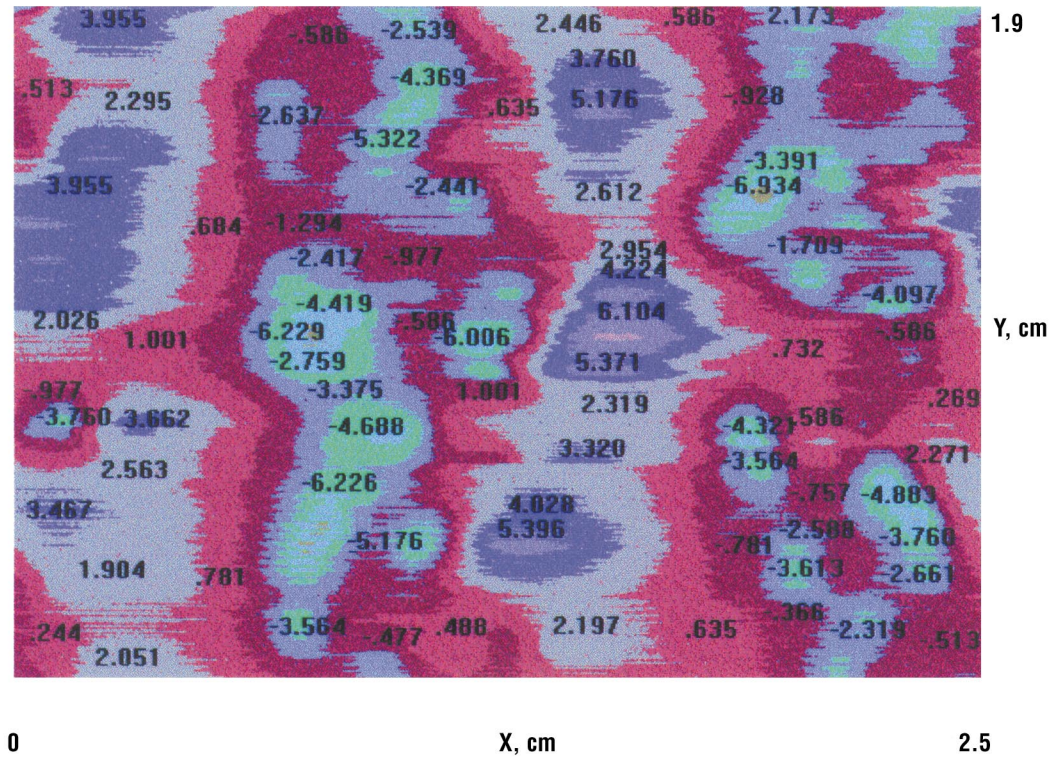


Figure 2. Initial localized corrosion in cast NASA-23 alloy.

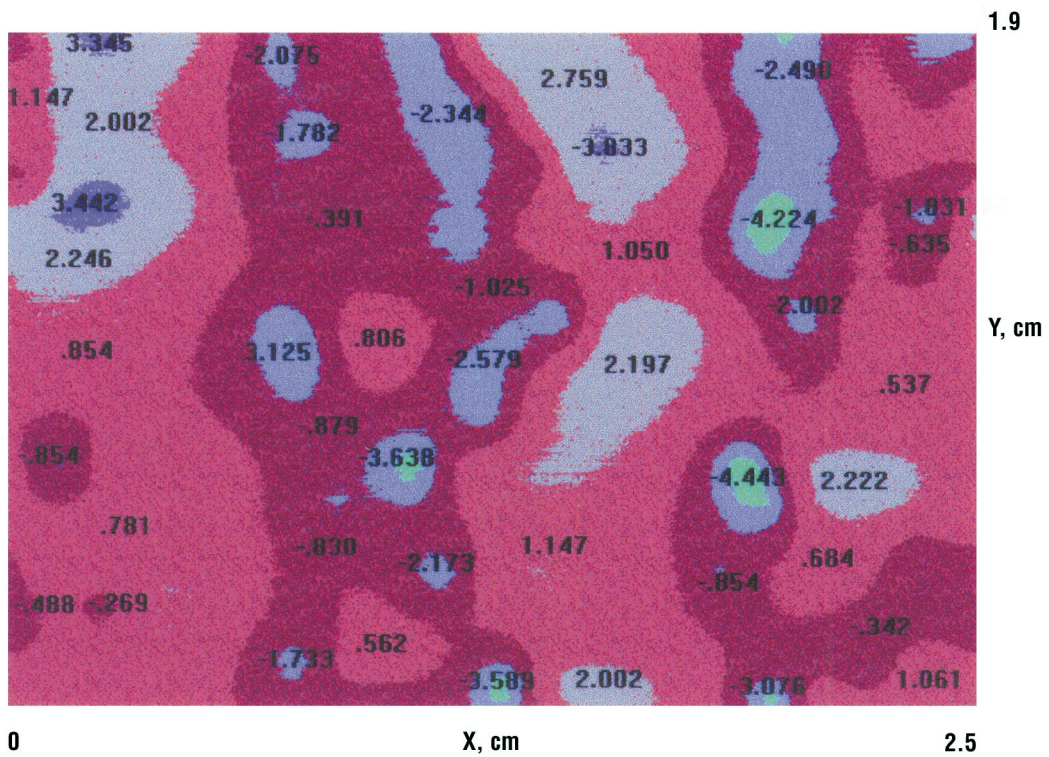


Figure 3. Localized corrosion in cast NASA-23 alloy after 1 hr.

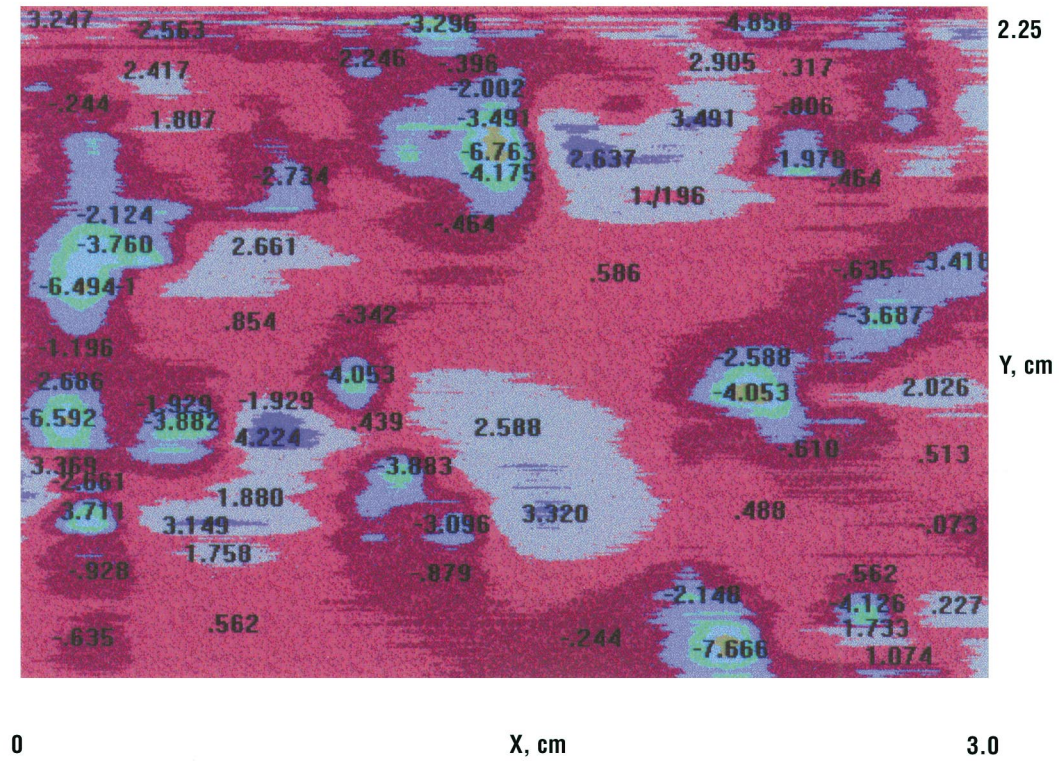


Figure 4. Initial localized corrosion in wrought NASA-23 alloy.

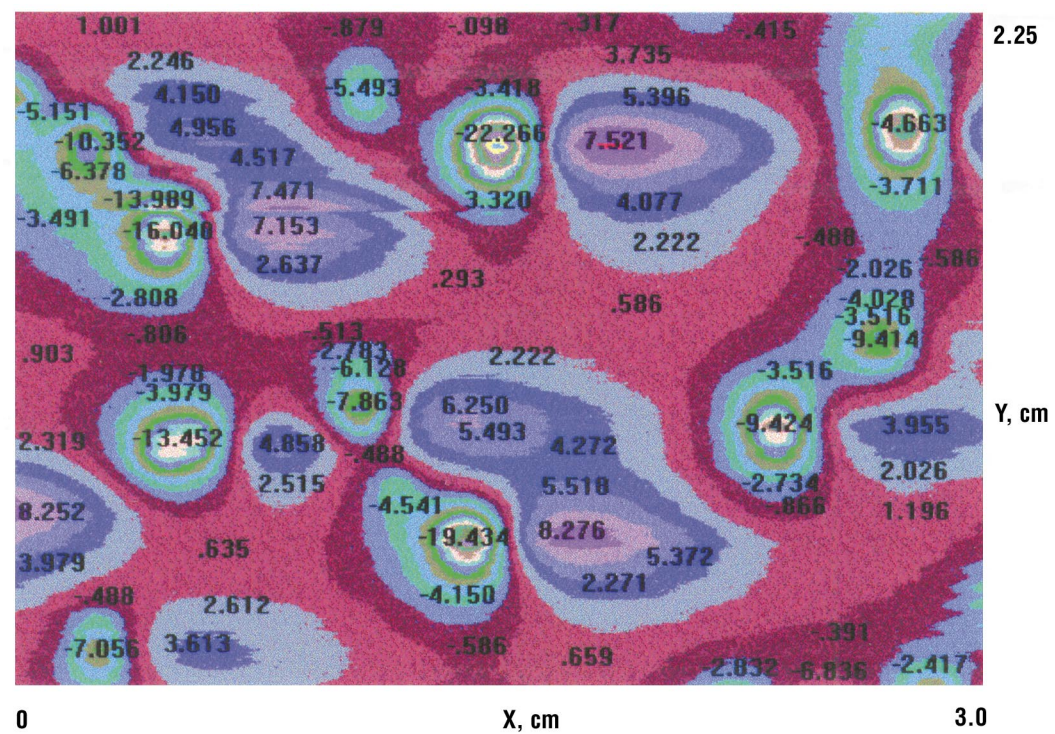


Figure 5. Localized corrosion in wrought NASA-23 alloy after 1 hr.

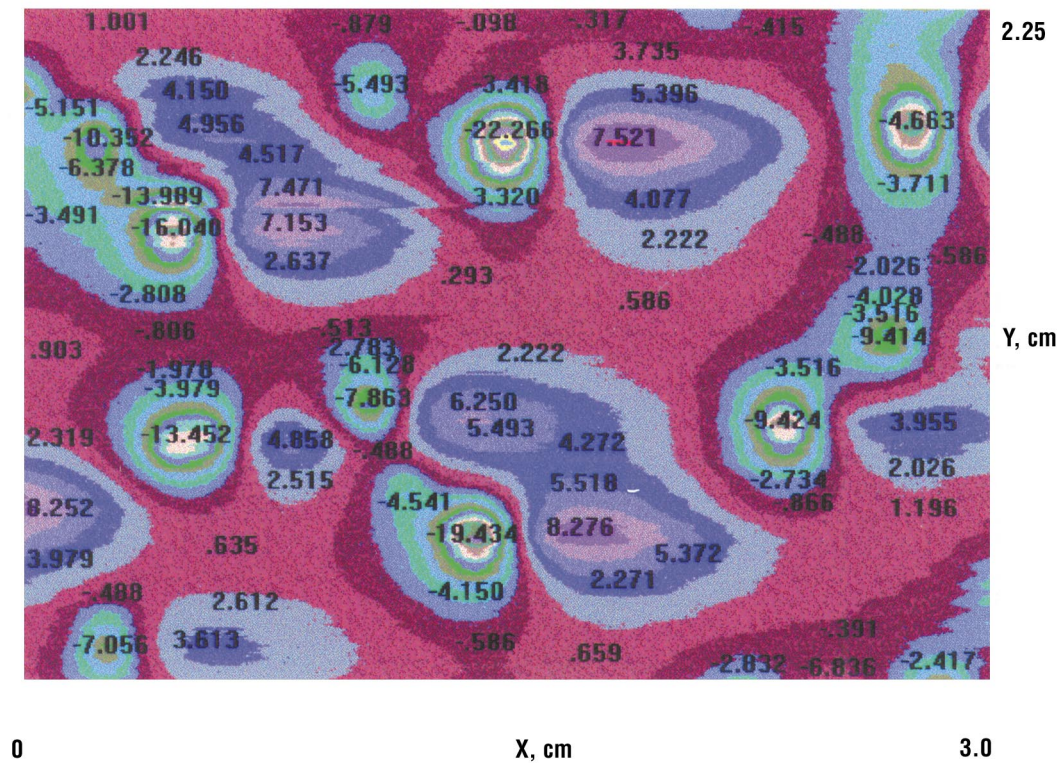


Figure 6. Localized corrosion in wrought NASA-23 alloy after 1 hr.

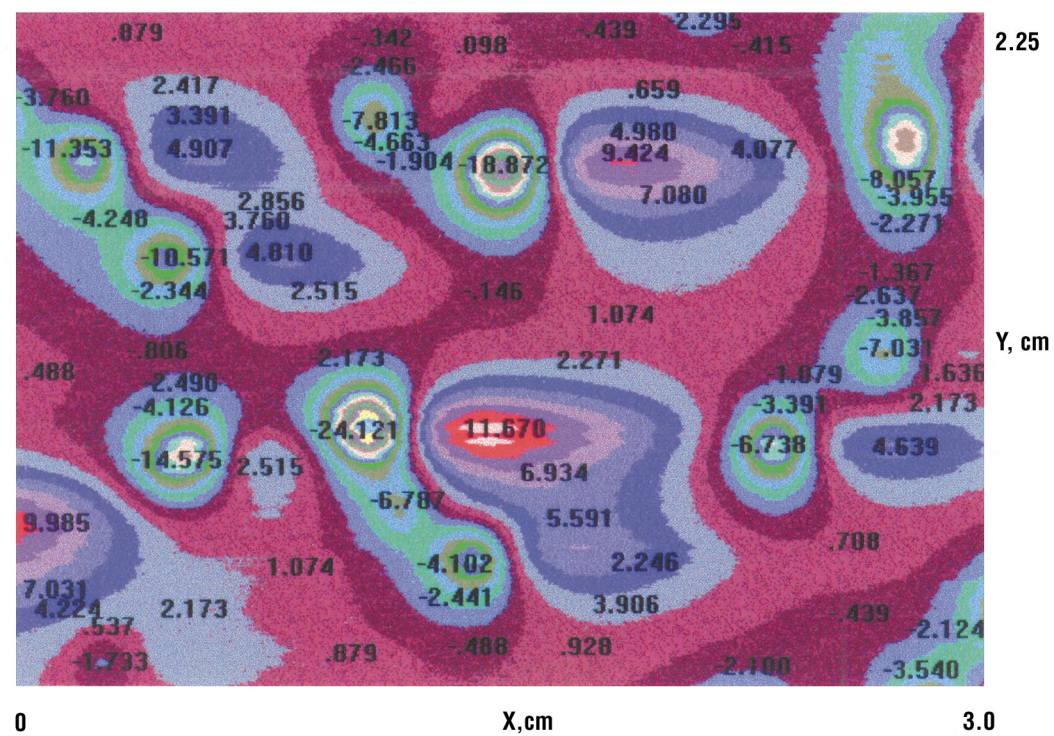


Figure 7. Localized corrosion in wrought NASA-23 alloy after 2 hr.

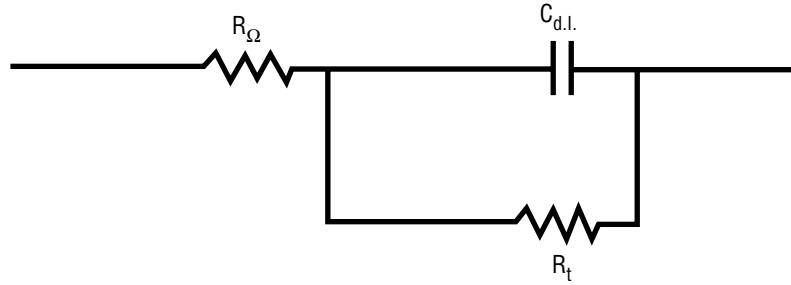


Figure 8. Circuit representing alternating current impedance response for bare metals.

The observed normal corrosion rates for the cast and wrought NASA-23 alloy, measured over a period of 10 days, are shown in figure 9. The curves generally are much the same for both the cast and wrought alloys for the first 6 days of data collection. However, the curve for the cast alloy deviates considerably from that for the wrought alloy for the last 2 days of measurement. The data point for the corrosion rate at 8 days was taken with the EIS method, while that for the corrosion rate at 10 days was taken using the PR method, so that both methods indicate an increased corrosion rate near the end of the 10-day period. It is possible that these points are the result of random deviations of the data, but it is believed that this is not the case. Indication is, however, that the corrosion rate may be decreasing after 8 days and again approaching that for the wrought alloy. The mean corrosion rate for the cast material was 0.003 mils per year (mpy) for the 10-day period, while that for the wrought alloy was 0.002 mpy; thus, the mean corrosion rates are about the same. The trend for the wrought material was toward a lower corrosion rate with time (-1.0×10^{-4} mpy/day), as determined by a linear regression technique, but the trend for the cast alloy was toward a higher corrosion rate with time (0.003 mpy/day). This difference is mostly due to the large deviation in corrosion rates observed for the cast alloy near the end of the 10-day period. However, as mentioned previously, the total current was decreasing for the cast alloy at the end of the 10-day period.

As mentioned in section 3, the maps for the cast and wrought alloys should be in accord with those observed in the corrosion rate measurements. However, it must be remembered that normal corrosion rates (with no applied potential) are quite low (about 0.003 mpy), while the maps were taken with the samples at a much higher potential (about 1 V) and at a very high corrosion rate. Initial map scans for the cast and wrought alloys (figs. 2 and 4, respectively) indicate that the features are stronger and more highly localized in the cast alloy than in the wrought alloy. Thus, the corrosion rates and trends observed in figure 9 over a 10-day period are in general agreement with the initial map scans observed in the case of the SRET experiments. Thus, the SRET experiments seem to predict the conditions (corrosion rates and trends) which would exist under normal corrosion rates after a long period of time.

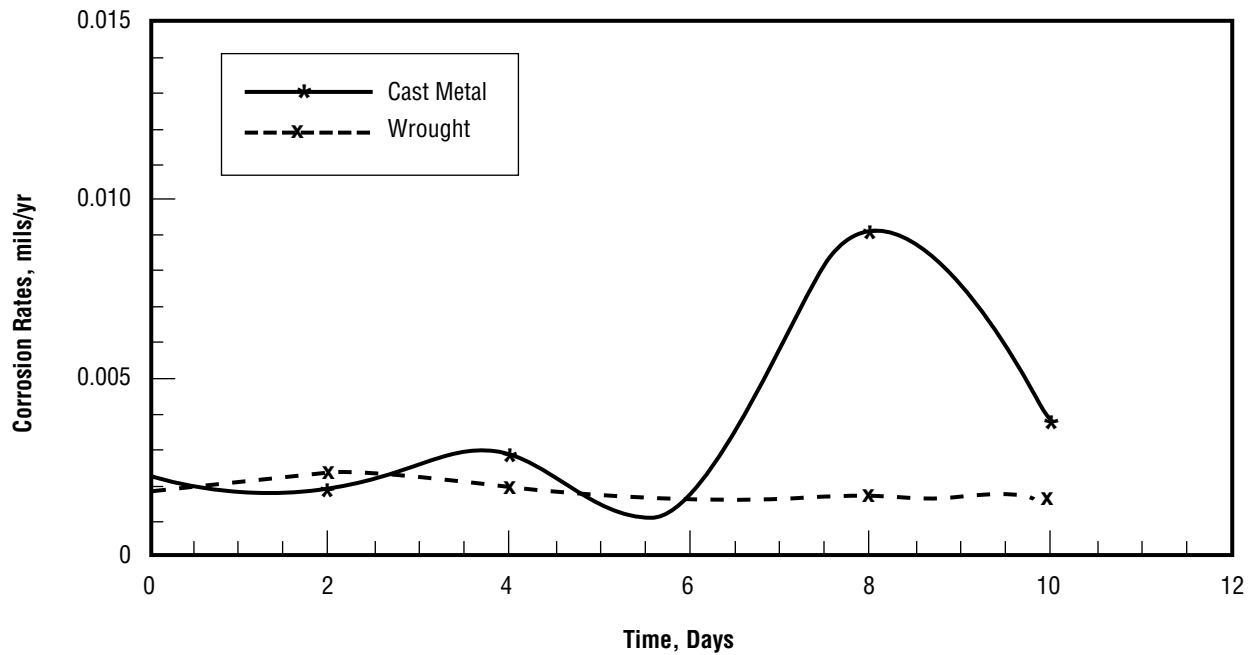


Figure 9. Observed corrosion rates for wrought and cast NASA-23 alloy.

5. CONCLUSIONS

The results of this study corroborate the findings of the stress corrosion study performed in 1994.¹ The corrosion rates of both wrought and cast NASA-23 are very low, and confirm the findings that the NASA-23 alloy is not susceptible to corrosion. The corrosion rates observed in this study were 0.002 mpy for the wrought material and 0.003 mpy for the cast material. These values are extremely low, and indicate that NASA-23 is not susceptible to corrosion. It is believed that differences in corrosion rates between the cast and wrought materials are due to differences in microstructure.

REFERENCES

1. Torres, P.D.; and Montano, J.W.: Internal Memorandum, EH24 (94–57), June 8, 1994.
2. Stern, M.; and Geary, A.L.: *Journal of the Electrochemical Society*, Vol. 102, p. 609, 1955.
3. Stern, M.; and Geary, A.L.: *Journal of the Electrochemical Society*, Vol. 104, p. 56, 1957.
4. Stern, M.: *Corrosion*, Vol. 14, p. 440t, 1958.
5. Knockemus, W.W.: Summer Faculty Research Fellow, Huntington College, Montgomery, AL, August 2, 1985.
6. Danford, M.D.: “Equivalent Circuit Models for AC Impedance Data Analysis,” *NASA Technical Paper 100402*, June 1990.
7. Gerchakov, S.M.; Udey, L.R.; and Mansfeld, F.: “An Improved Method for Analysis of Polarization Resistance Data.” *Corrosion*, Vol. 37, p. 696, 1981.

REPORT DOCUMENTATION PAGE			Form Approved OMB No. 0704-0188	
Public reporting burden for this collection of information is estimated to average 1 hour per response, including the time for reviewing instructions, searching existing data sources, gathering and maintaining the data needed, and completing and reviewing the collection of information. Send comments regarding this burden estimate or any other aspect of this collection of information, including suggestions for reducing this burden, to Washington Headquarters Services, Directorate for Information Operation and Reports, 1215 Jefferson Davis Highway, Suite 1204, Arlington, VA 22202-4302, and to the Office of Management and Budget, Paperwork Reduction Project (0704-0188), Washington, DC 20503				
1. AGENCY USE ONLY (Leave Blank)		2. REPORT DATE September 1997		3. REPORT TYPE AND DATES COVERED Technical Paper
4. TITLE AND SUBTITLE Corrosion Studies of Wrought and Cast NASA-23 Alloy			5. FUNDING NUMBERS	
6. AUTHORS M.D. Danford				
7. PERFORMING ORGANIZATION NAME(S) AND ADDRESS(ES) George C. Marshall Space Flight Center Marshall Space Flight Center, Alabama 35812			8. PERFORMING ORGANIZATION REPORT NUMBER M-838	
9. SPONSORING/MONITORING AGENCY NAME(S) AND ADDRESS(ES) National Aeronautics and Space Administration Washington, DC 20546-0001			10. SPONSORING/MONITORING AGENCY REPORT NUMBER NASA TP-3698	
11. SUPPLEMENTARY NOTES Prepared by Materials and Processes Laboratory Science and Engineering Directorate				
12a. DISTRIBUTION/AVAILABILITY STATEMENT Subject Category 26 Unclassified-Unlimited			12b. DISTRIBUTION CODE	
13. ABSTRACT (Maximum 200 words) Corrosion studies were carried out for wrought and cast NASA-23 alloy using electro-chemical methods. The scanning reference electrode technique (SRET), the polarization resistance technique (PR), and the electrochemical impedance spectroscopy (EIS) were employed. These studies corroborate the findings of stress corrosion studies performed earlier, in that the material is highly resistant to corrosion.				
14. SUBJECT TERMS corrosion of NASA-23; electrochemical methods; SRET, EIS, and PR methods; comparison with stress corrosion results			15. NUMBER OF PAGES 16	
			16. PRICE CODE A03	
17. SECURITY CLASSIFICATION OF REPORT Unclassified	18. SECURITY CLASSIFICATION OF THIS PAGE Unclassified	19. SECURITY CLASSIFICATION OF ABSTRACT Unclassified	20. LIMITATION OF ABSTRACT Unlimited	